Progress in Polymer Science 105 (2020) 101243

Contents lists available at ScienceDirect

Progress in Polymer Science

journal homepage: www.elsevier.com/locate/ppolysci

The swollen polymer network hypothesis: Quantitative models of hydrogel swelling, stiffness, and solute transport

Nathan R. Richbourg[a,e], Nicholas A. Peppas[a,b,c,d,e,*]

[a] Department of Biomedical Engineering, University of Texas, Austin, TX 78712, United States
[b] McKetta Department of Chemical Engineering University of Texas, Austin, TX 78712, United States
[c] Division of Molecular Therapeutics and Drug Delivery, College of Pharmacy, University of Texas, Austin, TX 78712, United States
[d] Departments of Surgery and Pediatrics, Dell Medical School University of Texas, Austin, TX 78712, United States
[e] Institute for Biomaterials, Drug Delivery, and Regenerative Medicine. University of Texas, Austin, TX 78712, United States

ARTICLE INFO

Article history:
Available online 11 May 2020

Keywords:
Hydrogel
Swollen polymer network
Rubberlike elasticity
Equilibrium swelling
Mesh size
Diffusion model

ABSTRACT

The introduction of the work Makromoleküle by Herman Staudinger in 1919 brings back an understanding of the very early days of polymer science when characterizing the molecular structure of exact networks was a main goal of research. Here, we present updates to a swollen polymer network hypothesis with a focus on hydrogel physical properties. We discuss the connections between hydrogel structure, swelling behavior, mechanical properties, and transport properties, including the most substantial developments since the original Flory-Rehner model (1944) of swollen polymer networks. In addition to analyzing well-established and recent contributions to the swollen polymer network hypothesis, we introduce novel amendments that combine the insights of existing models. We suggest that coordinating rubberlike elasticity theory, equilibrium swelling theory, and mesh size theory will help to develop a universal predictive model for swelling, stiffness, and solute diffusivities in a diverse array of hydrogel formulations.

Contents

* Corresponding author at: Department of Biomedical Engineering, University of Texas, Austin, TX 78712, United States.
E-mail address: peppas@che.utexas.edu (N.A. Peppas).

https://doi.org/10.1016/j.progpolymsci.2020.101243
0079-6700/

Nomenclature

G	Shear modulus
ν	Total number of polymer chains
R	Ideal gas constant
T	Absolute temperature
$\overline{M}_c$	Number average molecular weight between crosslinks in a polymer network
$\overline{M}_n$	Number average molecular weight of an uncrosslinked polymer
φ_s	Polymer volume fraction in the swollen equilibrium state
χ	Flory-Huggins polymer-solvent interaction parameter, chemical potential form
V_1	Molar volume of the solvent
ρ_d	Dry density of the polymer network
ω	Cycle rank of a polymer network
f	Junction functionality in a polymer network
ΔG_{ph}	Elastic free energy change in a phantom-like network
I_1	First invariant of deformation
PEG	Poly(ethylene glycol)
PEGDA	Poly (ethylene glycol) diacrylate
RENT	Real elastic network theory
ν_{eff}	Elastically effective number of polymer chains in an imperfect network
ν_{tot}	Total number of polymer chains in an imperfect network
γ	Frequency of chain-end defects
$\Delta G_{ph,ce}$	Elastic free energy change in a phantom-like network with chain-end defects
V_d	Volume of the polymer network in the dried state
ΔG_{el}	Elastic component of free energy change due to equilibrium swelling
V_s	Volume of the swollen polymer network in the swollen equilibrium state
V_r	Volume of the swollen polymer network in the relaxed state
$\Delta \mu_{el}$	Elastic component of the chemical potential change due to equilibrium swelling
n_1	Number of solvent molecules in the swollen polymer network
φ_r	Polymer volume fraction in the relaxed state
ΔG_{el+def}	Elastic free energy change due to both swelling and applied deformation
ΔG_{def}	Elastic free energy change due to applied deformation
$I_{1,\,def}$	The first invariant of deformation for applied deformation
W	Strain-energy density function
ΔG_{tot}	Total free energy change
ΔG_{mix}	Mixing component of free energy change
$\Delta \mu_{tot}$	Total chemical potential change due to equilibrium swelling
$\Delta \mu_{mix}$	Mixing component of the chemical potential change due to equilibrium swelling
$\bar{\chi}$	Flory-Huggins polymer-solvent interaction parameter, free energy form
χ	Flory-Huggins polymer-solvent interaction parameter, chemical potential form
φ	Polymer volume fraction (in general)
χ_0	Zeroth polymer-solvent interaction parameter coefficient, chemical potential form
χ_1	First polymer-solvent interaction parameter coefficient, chemical potential form
k_b	Boltzmann thermodynamic constant
PVA	Poly(vinyl alcohol)
$\Delta \mu_{ion}$	Ionic component of the chemical potential difference
c^-_{gel}	Concentration of negative ions within the hydrogel
c^+_{gel}	Concentration of positive ions within the hydrogel
c^-_{sol}	Concentration of negative ions in the solution
c^+_{sol}	Concentration of positive ions in the solution
$c^-_{m,gel}$	Concentration of mobile negative ions within the hydrogel
$c^+_{m,gel}$	Concentration of mobile positive ions within the hydrogel
$c^-_{m,sol}$	Concentration of mobile negative ions in the solution
$c^+_{m,sol}$	Concentration of mobile positive ions in the solution
I	Ionic strength
$c^-_{polymer,\,gel}$	Concentration of polymer-associated negative ions in the hydrogel
i	Degree of ionization of the polymer repeating unit
M_r	Molecular weight of the polymer repeating unit
PAA	Poly(acrylic acid)
PDEAEMA	Poly(diethylaminoethyl methacrylate)
K_a	Acid dissociation constant
pH	Power of hydrogen or hydronium ion concentration ratio in aqueous solution
K_b	Base dissociation constant
pOH	Power of hydroxide ion concentration ratio in aqueous solution
FRAP	Fluorescence recovery after photobleach
FCS	Fluorescence correlation spectroscopy
FITC	Fluorescein isothiocyanate
ξ	Average mesh size of the polymer network
l	Polymeric carbon-carbon bond length
C_n	Polymer-specific characteristic ratio for a chain of n repeating units
C_∞	Polymer-specific characteristic ratio for a long chain
λ	Polymer backbone bond factor
$\bar{l}$	Weighted average of polymeric backbone bond lengths per repeating unit

r_s	Stokes hydrodynamic radius of the solute
η	Viscosity of the solvent
D_0	Diffusivity coefficient of the solute in free solution
Y	Scale factor for the free volume-normalized volume displacement of diffusion
D	Effective diffusivity coefficient of the solute within the swollen polymer network
r_f	Radius of a polymer fiber in a polymer network
PALS	Positron annihilation lifetime spectroscopy
r_{FV}	Average radius of a free volume void
r_{FVW}	Average radius of a free volume void in pure water
PPEGMA	Poly(poly(ethylene glycol) methacrylate)
χ_{gel}	Polymer-solvent interaction parameter for a chain in a polymer network
χ_{sol}	Polymer-solvent interaction parameter for a free polymer chain in solution
a_1	Chemical activity of the solvent
MSDM	Multiscale diffusion mod

1. Introduction

1.1. Modeling hydrogels as swollen polymer networks

Hydrogels are polymer networks that swell and maintain their structure in the presence of water [1]. Their applications include biosensing [2,3], controlled drug release [4,5], and regenerative medicine [6,7]. To improve hydrogel physical and chemical properties for each of these applications, ongoing synthetic work has expanded the choices of polymer and crosslinking agent used in hydrogels as well as the mechanisms for forming a network [8]. These advances motivate improvements to fundamental models of the relationship between polymer network structure and function. Quantitative models that relate function to structure efficiently represent trends in experimental observations and provide generalized explanations for interactions that are too complex to analyze in a single experiment. However, the established quantitative models that relate hydrogel structure to physical properties include inappropriate assumptions for many current hydrogel formulations. For example, the Flory-Rehner equation assumes that all network junctions are tetrafunctional [9], but junction functionalities range from a minimum of three up to tens or hundreds of polymer chains converging to one point [8].

Despite their limiting assumptions, fundamental structure-property models such as the Flory-Rehner equation facilitate iterative development. By testing the assumptions and developing case-specific amendments to the models, researchers have adapted the fundamental models to their various needs and applications. Unfortunately, the proliferation of case-specific equations has limited universal coordination between models and comparison between different hydrogel systems. In this work, we propose a comprehensive set of coordinated amendments to the models relating hydrogel structure to swelling, stiffness, and solute diffusivity. We call this set of amendments the *swollen polymer network hypothesis* to acknowledge its current lack of validation, but we anticipate that the hypothesis will clarify which modeling assumptions need further investigation and ultimately contribute toward increased precision and efficiency in designing biomedically relevant hydrogel systems.

1.2. Three fundamental theories of swollen polymer networks

The swollen polymer network hypothesis coordinates three fundamental theories relating swollen polymer network structure to physical properties. Rubberlike elasticity theory relates structure to stiffness, equilibrium swelling theory relates structure to swelling in solvent, and mesh size theory relates structure to solute diffusivity within the swollen network.

Rubberlike elasticity theory suggests that a stiffness of a polymer network derives from the entropy lost as coiled polymer chains in the network extend and reduce their number of available conformations [10]. Treloar's estimation of shear modulus from the number of chains in a polymer network (Eq. (1)) [11] makes rubberlike elasticity theory testable on any polymer network under any form of applied deformation, but practical application to hydrogels requires corrections for swollen polymer networks, non-tetrafunctional networks, and network imperfections. These corrections are addressed in section 2.

$$G = \nu RT \tag{1}$$

In Eq. (1), G is the polymer network's shear modulus, ν is the number of chains in the polymer network, R is the ideal gas constant, and T is the absolute temperature of the system.

Equilibrium swelling theory estimates the amount of solvent contained in a swollen polymer network at equilibrium based on independent free energy contributions [7]. The first quantitative model of equilibrium swelling theory, the Flory-Rehner equation (Eq. (2)), compares entropic contribution of mixing polymer and solvent with the elastic energy created as the polymer network swells to incorporate solvent [12,13]. Section 3 updates the Flory-Rehner model of equilibrium swelling to apply to a broader set of hydrogel systems, including hydrogels with ionic side-chains, hydrogels crosslinked in the present of solvent, and hydrogels where the polymer-solvent interaction parameter varies with polymer volume fraction.

$$\frac{1}{\overline{M}_c} = \frac{2}{\overline{M}_n} - \frac{\ln(1-\varphi_s) + \varphi_s + \chi\varphi_s^2}{V_1\rho_d[\varphi_s^{\frac{1}{3}} - \frac{\varphi_s}{2}]} \tag{2}$$

In Eq. (2), $\overline{M}_c$ is the average molecular weight between crosslinks, $\overline{M}_n$ is the average molecular weight of the polymer chains prior to crosslinking, φ_s is the polymer volume fraction at swelling equilibrium, χ is the polymer-solvent interaction parameter, V_1 is the molar volume of the solvent, and ρ_d is the dry density of the polymer network.

Mesh size theory uses swollen polymer network structure properties to estimate how much solute diffusivity coefficients are reduced within a hydrogel [14]. Swollen polymer networks reduce solute diffusivity based on the polymer volume fraction, which indicates the likelihood of a solute colliding with a polymer chain, and the distance between two connected junctions (the hydrogel's mesh size), which influences whether a network loop is large enough for the solute to pass through it [15]. Competing models of mesh size theory emphasize different aspects of the interactions between solute, solvent, and polymer network, leading to conflicting estimations of solute diffusivity [16]. These theoretical differences have been magnified by differences in the experimental techniques used to measure solute diffusivity in hydrogels [17–19]. Further development toward a universal model of mesh size theory will require simultaneous theoretical and experimental progress. Section 4 on mesh size theory includes updates on how to estimate mesh size from other structural parameters, commentary on the development of mesh size models and the associated experimental techniques, and arguments for additional structural considerations to be included in future models of mesh size theory.

The swollen polymer network hypothesis suggests that rubberlike elasticity theory, equilibrium swelling theory, and mesh size theory are fundamentally linked in swollen polymer networks. Indeed, all three have been used to estimate the average molecular weight between crosslinks of a swollen polymer network [20,21].

Therefore, one should be able to use data from swelling, stiffness, or solute diffusivity in a hydrogel to predict the other two properties for that hydrogel. However, before this ideal predictive tool for hydrogel physical properties can be fully realized, each theory must be coordinated using consistent parameters and thoroughly cross validated. The swollen polymer network hypothesis takes the first step toward developing a robust universal model for hydrogel design by providing a united framework for three fundamental theories of structure-property relationships in hydrogel systems.

2. Rubberlike elasticity theory

2.1. Hydrogels behave as phantom-like networks

Although initially developed for solvent-free rubber networks, rubberlike elasticity theory has contributed to an understanding of the mechanical properties of hydrogels. Erman and Mark [10] summarized many aspects of rubberlike elasticity applied to swollen polymer networks with significant updates to the fundamental work of Flory and Treloar in *Structures and Properties of Rubberlike Networks*. Their discussion centered on the role of entanglements and junction motion in deformed polymer networks, often described in the conflicting affine and phantom deformation models. The affine network model, used in the Flory-Rehner equation, suggests that all junction points move in proportion to the macroscopic deformation. As a result, all macroscopic deformation can be attributed to chain extension. Flory defended the use of the affine network model by arguing that a dense network of polymer chains would entrap the junction so that it would not move without associated macroscopic deformation [22]. In contrast, the phantom network model developed by James and Guth [23,24] treats junctions as phantom structures that move independently of chains. With a phantom network, some of the macroscopic deformation changes the relative position of junctions, resulting in the individual chains extending to a lesser extent than the total macroscopic deformation.

Erman and Mark [10] unified the inconsistencies between affine and phantom deformation models with the constrained junction model of Deam and Edwards [25], which interprets the transition between affine and phantom deformation models as the effect of chain entanglements constraining the motion of network junctions. This model provides a generalized tool for evaluating the effects of entanglement in polymer network mechanics, but the resulting parameters are too context-specific for general application to swollen polymer networks. However, the constrained-junction model presents evidence that the phantom model is more appropriate for swollen networks than the affine model. Because hydrogels swollen to equilibrium typically reach less than 20 % polymer volume fraction, the resulting low concentration of entanglement points facilitates greater motion of junction points. Furthermore, many hydrogels are synthesized from polymer chains in aqueous solution. Compared to a melt state, polymer chains in aqueous solution are much less likely to be entangled prior to crosslinking, reducing the number of permanent entanglements in the resulting polymer network. Based upon the entanglement-driven interpretation of the constrained junction model, the phantom network does not fully capture the deformation behavior of swollen polymer networks, but it is a better approximation than the affine network model.

Transitioning from the affine network model to the phantom network model results in the free energy of deformation scaling with cycle rank (ω) instead of the number of polymer chains (Eq. (3)). The full derivation for this replacement is available elsewhere [10]. Cycle rank, originally used in graph theory, describes the number of connections that need to break to render a network acyclic (Fig. 1A). In a large, highly connected hydrogel network, the cycle rank requires both junction functionality (f) and the number of chains (Eq. (4)). The junction functionality term in Eq. (4) accounts for how junction motion in a phantom network reduces the stretch experienced by each chain. A network's junction functionality is the number of chains that converge at each network junction [26].

$$\Delta G_{ph} = \frac{1}{2}\omega RT[I_1 - 3] \tag{3}$$

In Eq. (3), ΔG_{ph} is the free energy change due to deformation based on a phantom network model and I_1 is the first invariant of deformation.

$$\omega = \left(1 - \frac{2}{f}\right)\nu \tag{4}$$

The relationship between cycle rank, junction functionality, and the number of chains in a polymer network extends the applicability of rubberlike elasticity theory. Substituting Eq. (4) into Eq. (3) shows that free energy scales linearly with the number of chains even when using the phantom network model. With respect to overall trends, results obtained using the affine network model are not invalidated by the inclusion of junction functionality. Furthermore, accounting for junction functionality as an independent parameter corrects the assumption of tetrafunctional networks, which does not apply to many hydrogel systems such as multi-arm poly(ethylene glycol) (PEG) hydrogels [27], end-linked systems such as poly(ethylene glycol) diacrylate (PEGDA) hydrogels [28], and dendrimer-crosslinked hydrogels [29] (Fig. 1B).

However, the influence of junction functionality decreases with increasing junction functionality, with the limit as junction functionality approaches infinity rendering the phantom network model indistinguishable from the affine network model (Fig. 1C). This result is theoretically consistent with understanding that the motion of a junction with more polymer chains attached will be more restricted with respect to the motion of the polymer chains. Taken together, the effects of including junction functionality in rubberlike elasticity theory through the phantom network model greatly increases the nuance and range with which the theory can be studied and applied in hydrogel systems.

2.2. Modeling imperfect swollen polymer networks

Rubberlike elasticity theory-based models start with an assumption of perfect polymer networks and therefore do not account for defects that occur in the formation of real polymer networks. Real network defects tend to fall under three categories: permanent entanglement defects, loop defects, and chain-end defects. Permanent entanglement defects are addressed in the constrained-junction model of Deam and Edwards [25] that helped to justify use of a phantom model for swollen polymer networks.

Loop defects form when a polymer chain interacts twice with one junction or when two or more chains are attached to the same two functional groups, creating local inconsistencies in hydrogel mechanical properties. Ongoing work by Johnson and colleagues to address the effects of loop defects using real elastic network theory (RENT) have shown that loops that include three or more network junctions do not cause significant deviations from the network model [8,30,31]. Full application of RENT in swollen polymer networks would lead to an improved model for the swollen polymer network hypothesis, but it is not clear if RENT can be universally applied to all the crosslinking schemes that the swollen polymer network hypothesis aims to address.

Chain-end defects represent a break in the polymer chain connecting two junctions, which can result from termination in the synthesis of radically polymerized networks, chemical degradation of a chain in the network, or as a predictable result of the precursor polymer molecular weight in vulcanization-type network synthe-

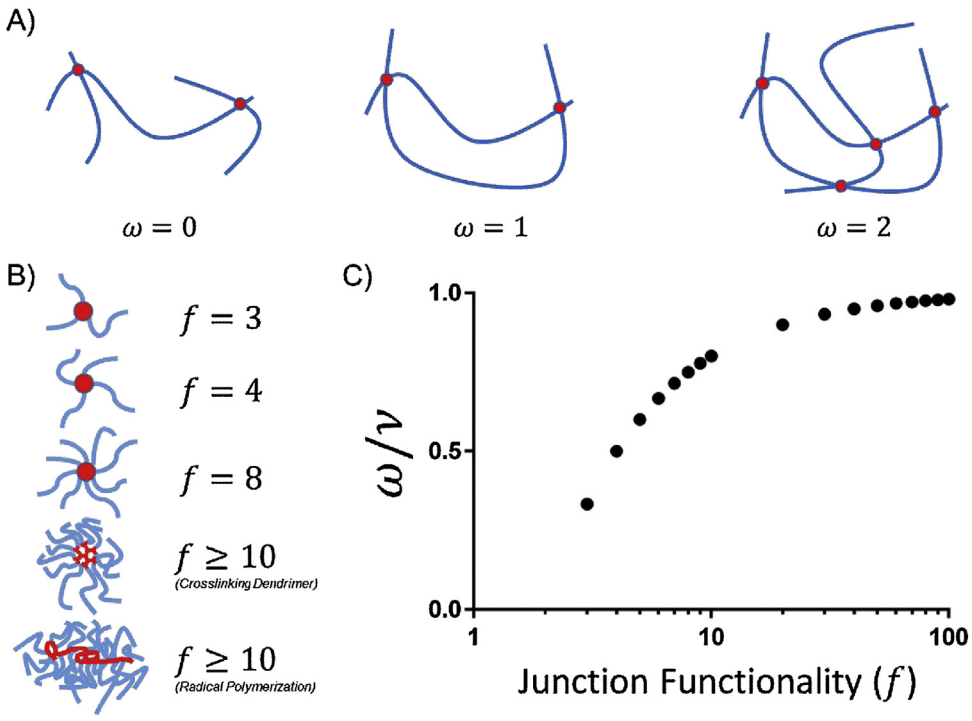

Fig. 1. Under the phantom network model of rubberlike elasticity theory, cycle rank (ω) and junction functionality (f) modulate the effect of the number of polymer chains (ν) on a hydrogel's stiffness. A) Schematic representation of increasing cycle rank in simplified polymer networks. B) Schematic representation of junction functionality, where red regions represent a network junction and blue lines represent the attached polymer chains. As junction functionality increases, more polymer chains connect at each junction. C) As junction functionality increases, the difference between cycle rank and the number of polymer chains decreases, asymptotically converging as junction functionality approaches infinity. As a result, the phantom network model becomes indistinguishable from the affine network model at high junction functionality.

ses. Flory included a correction term for the third case of chain-end defects in the Flory-Rehner equation and later updated the term for non-tetrafunctional junctions (Eq. (5)) [9,32]. Flory's correction term differentiates between the elastically effective number of chains (ν_{eff}) and the total number of chains (ν_{tot}) in an imperfect polymer network. When updating rubberlike elasticity models to account for network imperfections, the elastically effective number of chains replaces the ideal number of chains in terms of strain energy, but the total number of chains still describes the total polymer mass in the hydrogel.

$$\nu_{eff} = \left(1 - \frac{f\bar{M}_c}{(f-2)\bar{M}_n}\right)\nu_{tot} \tag{5}$$

Eq. (5) has been indiscriminately misapplied through use of the Flory-Rehner equation with crosslinking schemes other than random side-group crosslinking of precursor polymer chains [28,33]. To help correct such misuse, we propose a generalized term, the frequency of chain-end defects (γ) (Eq. (6)). With a generalized frequency of chain-end defects, the value can be calculated independently for each crosslinking scheme. For example, the frequency of chain-end defects in multi-arm PEG hydrogels could be estimated based on the stoichiometry of PEG-bound functional groups to crosslinking agent functional groups. Combining the generalized frequency of chain-end defects term with the phantom network model update and converting the total number of polymer chains to standard, measurable terms yields a general equation for rubberlike elasticity in hydrogel systems (Eq. (7))

$$\nu_{eff} = (1-\gamma)\,\nu_{tot} \tag{6}$$

$$\Delta G_{ph,ce} = \frac{1}{2}RT\left(1 - \frac{2}{f}\right)(1-\gamma)\frac{V_d\rho_d}{\bar{M}_c}\left[I_1 - 3\right] \tag{7}$$

In Eq. (7), $\Delta G_{ph,ce}$ represents the free energy of elastic deformation in phantom-like networks with chain-end defects and V_d represents the dry volume of the polymer network.

2.3. Rubberlike elasticity in equilibrium swelling theory

As hydrogels swell to incorporate water, the polymer chains in the network pull on each other, creating a net elastic energy described by rubberlike elasticity theory. For the elastic free energy transition of swelling to equilibrium, the relaxed state, in which no force propagates through the network chains, must be defined. According to the Peppas-Merrill model of equilibrium swelling, the relaxed state immediately follows crosslinking [20,34]. If the polymer volume fraction remains unchanged during the crosslinking process, polymer chains are unlikely to stretch and accumulate elastic energy (Fig. 2). Notably, this definition of the relaxed state facilitates the application of rubberlike elasticity theory and equilibrium swelling theory to hydrogels crosslinked in the presence of solvent. Subsequent state changes such as swelling to equilibrium in excess solvent or drying to remove all solvent stretch the polymer network and change the elastic energy within the network. Therefore, the change in volume or polymer volume fraction as a hydrogel swells from the relaxed state to the swollen equilibrium state defines the elastic free energy change (Eq. (8)).

$$\Delta G_{el} = \frac{1}{2}RT\left(1 - \frac{2}{f}\right)(1-\gamma)\frac{V_d\rho_d}{\bar{M}_c}\left[3\left(\frac{V_s}{V_r}\right)^{\frac{2}{3}} - 3\right] \tag{8}$$

In Eq. (8), ΔG_{el} is the free energy change of elastic deformation due to hydrogel swelling, V_s is the volume of the equilibrium-swollen hydrogel and V_r is the volume of the hydrogel in the relaxed state.

To obtain the elastic chemical potential change ($\Delta\mu_{el}$) with respect to the number of water molecules, we assume that the

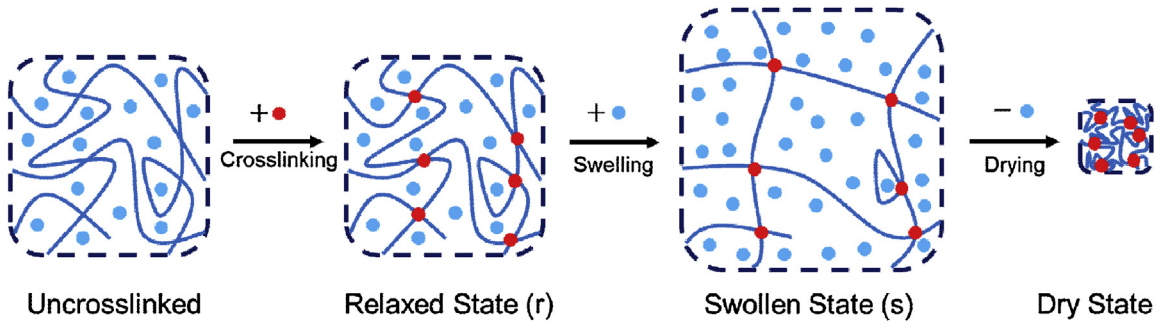

Fig. 2. Schematic of relevant state changes in hydrogel swelling. In the uncrosslinked state, chains are not connected and therefore cannot exert force on each other. Crosslinking results in a relaxed state as long as the polymer volume fraction remains unchanged. The addition of excess solvent drives swelling to free energy equilibrium. For calculation of polymer volume fraction, a final drying step enables accurate measurement of the polymer network's mass and volume.

polymer and solvent are incompressible (Eq. (9)) and partially differentiate the free energy equation with respect to the number of solvent molecules (n_1) at equilibrium. Converting from volumes to polymer volume fractions yields Eq. (10).

$$V = V_d + n_1 \frac{V_1}{N_A} \tag{9}$$

$$\Delta\mu_{el} = RT\left(1 - \frac{2}{f}\right)(1-\gamma)\frac{V_1\rho_d}{\overline{M}_c}\varphi_r^{\frac{2}{3}}\varphi_s^{\frac{1}{3}} \tag{10}$$

In Eq. (10), φ_r represents the polymer volume fraction in the relaxed state.

The elastic chemical potential change derived here for imperfect phantom-like polymer networks synthesized in the presence of solvent will update the equilibrium swelling model in section 3.

2.4. Applied deformation of swollen polymer networks

In addition to the elastic component of equilibrium swelling, rubberlike elasticity theory generally addresses how much a swollen polymer network stretches in response to externally applied forces. The elastic free energy change of deforming a swollen polymer network derives from Eq. (7), but the elastic free energy change of swelling to equilibrium (defined by Eq. (8)) and from the relaxed state (ΔG_{el+def}) must be considered to accurately determine the free energy change upon deformation from the swollen state (ΔG_{def}) (Eq. (11)).

$$\Delta G_{el+def} - \Delta G_{el} = \Delta G_{def} \tag{11}$$

The total deformation from the relaxed state is the product of the externally applied deformation (generalized as $I_{1,def}$) and the deformation from swelling. Evaluating the free energy of externally applied deformation as the difference between total deformation and the swelling deformation introduces a swelling-based scaling term $\left(V_s/V_r\right)^{\frac{2}{3}}$ that would not have been included by naively replacing I_1 in Eq. (7) with $I_{1,def}$ (Eq. (12)).

$$\Delta G_{def} = \frac{1}{2}RT\left(1 - \frac{2}{f}\right)(1-\gamma)\frac{V_d\rho_d}{\overline{M}_c}\left(\frac{V_s}{V_r}\right)^{\frac{2}{3}}[I_{1,def} - 3] \tag{12}$$

If the externally applied deformation does not change the total volume of the hydrogel, the free energy change can be converted to a strain-energy density function (W) by dividing by the volume of the swollen polymer network. Ratios of dry, swollen, and relaxed state volumes then convert to polymer volume fractions (Eq. (13)). Comparison with the general Neo-Hookean strain-energy density function shows that rubberlike elasticity theory describes a special case of the Neo-Hookean hyperelastic model, giving a structural rational behind the phenomenological shear modulus parameter (G). Ultimately, the shear modulus and therefore the force needed to stretch a hydrogel can be estimated based on hydrogel swelling data and structural parameters (Eq. (14)) [35]. Eq. (14) significantly updates Eq. (1) to provide precise predictions of elastic behavior in real phantom-like swollen polymer networks.

$$W = \frac{1}{2}RT(1 - \frac{2}{f})(1-\gamma)\frac{\rho_d}{\overline{M}_c}\varphi_r^{\frac{2}{3}}\varphi_s^{\frac{1}{3}}[I_{1,def} - 3] \tag{13}$$

$$G = RT(1 - \frac{2}{f})(1-\gamma)\frac{\rho_d}{\overline{M}_c}\varphi_r^{\frac{2}{3}}\varphi_s^{\frac{1}{3}} \tag{14}$$

2.5. Current limitations of rubberlike elasticity theory

Despite the advances in model development described in the previous sections, further limitations of rubberlike elasticity theory emerge from idealistic assumptions about the polymer chain and its interactions with the environment [9–11,36,37]. Rubberlike elasticity theory systematically neglects the effects of each polymer chain's length and molecular structure. While convenient for modeling, these assumptions completely eradicate the possibility for accurately analyzing the reasons behind differences in real polymer networks. Instead, any influences from chain length distribution, polymer chain stiffness, or higher-order bonding is instead misallocated within the model, most often resulting in systematically erroneous predictions of $\overline{M}_c$.

While the ideal polymer network is uniform in terms of chain lengths, all the models described here have also shown to be applicable to networks with a narrow Gaussian distribution of chain lengths. However, the analysis becomes more complicated as the distribution spreads or becomes non-Gaussian altogether, especially since non-Gaussian chain length distributions result in non-Gaussian end-to-end length distributions and ultimately disrupt the generalized function for the change in available conformations as a polymer chain is extended [38]. Experimentally, hydrogels synthesized with bimodal chain length distributions create stronger, more durable networks [10], but this result cannot yet be explained or captured within a fundamental model without invalidating the assumption of Gaussian chain length distribution.

Another requirement of the current rubberlike elasticity models is that the contour length or fully extended length of each polymer chain must be far greater than the end-to-end chain length. This requirement is again associated with the available conformations function because the available conformations drop much more rapidly as the polymer approaches its maximum extension. Experimentally, this assumption contributes to deviations from modeled

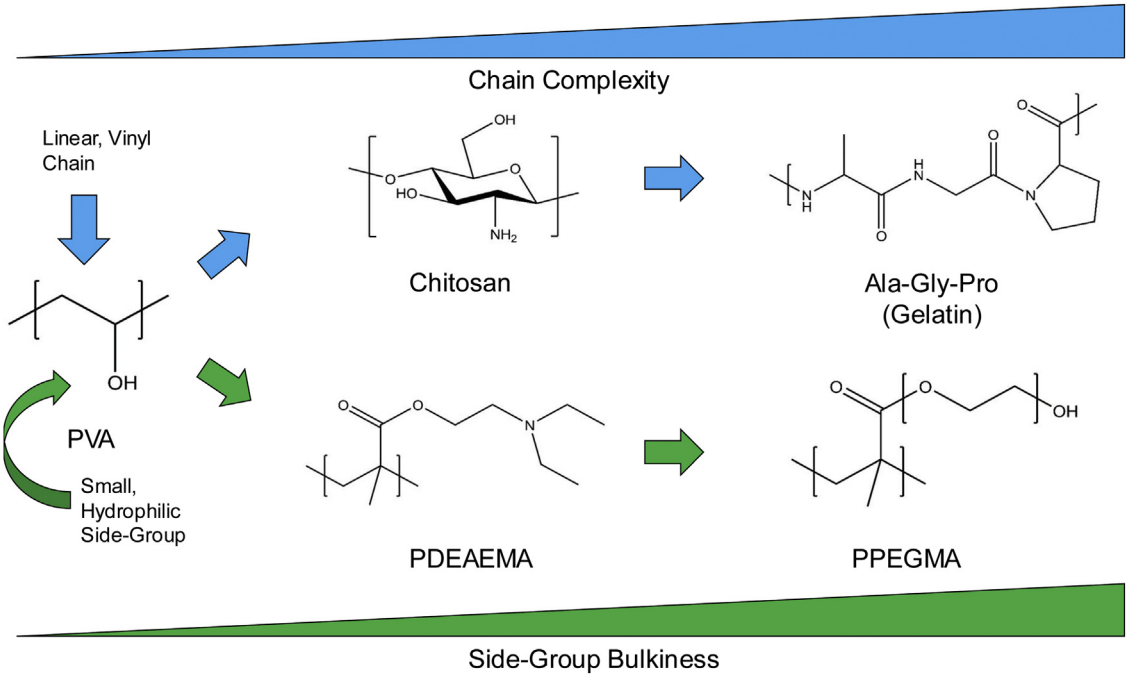

Fig. 3. Increases in chain complexity and side-group bulkiness cause deviation from ideal polymer statistical mechanics. Poly(vinyl alcohol) (PVA) is an ideal hydrogel polymer. Biopolymers such as chitosan and gelatin (represented here by the frequently occurring tripeptide alanine-glycine-proline) have increased chain complexity with nonlinear chains and higher-order interactions along the polymer structure. These complications reduce the probable chain configurations in the entropic spring model. Poly(diethylaminoethyl methacrylate) (PDEAEMA) and poly(poly(ethylene glycol) methacrylate) (PPEGMA) have increasingly bulky side chains that contribute steric hindrance and friction to polymer dynamics. These effects have not been addressed in quantitative hydrogel models.

values at high extensions as well as with highly crosslinked systems that have short chain lengths.

According to Erman and Mark [10], the strain energy density function of a polymer network does not change based on the chemical structure of the polymer's repeating unit. However, bulky sidechains and highly grafted chains, nonlinear covalent bond structures such as those found in sugars, and functional groups capable of higher-order interactions all contribute to deviations from the ideal entropic chain thermodynamics in real polymer networks (Fig. 3). As with the constrained junction model, attempts to quantitatively incorporate these effects into rubberlike elasticity models lead to unwieldy series approximations [10,37]. However, the failure to account for these differences limits the ability to compare different polymer systems. Further development of fundamental models of hydrogel mechanics will need to address the

hortcomings of rubberlike elasticity theory. A comprehensive mechanical model must account for the effects of chain length, non-Gaussian distributions, and structure-dependent flexibility, especially since these influences are becoming more significant within the expanding repertoire of hydrogel systems.

3. Equilibrium swelling theory

3.1. Free energy and chemical potential

Equilibrium swelling theory compares the thermodynamic effects of adding more solvent into a swellable polymer network, which can be found by partially differentiating each contribution to free energy with respect to the number of solvent molecules (n_1) (Eq. (15)). When the total chemical potential ($\Delta\mu_{tot}$) is zero, the net flux of solvent molecules in and out of the system is zero, resulting in the equilibrium swelling state

$$\frac{\partial(\Delta G_{tot})}{\partial n_1} = \frac{\partial(\Delta G_{mix})}{\partial n_1} + \frac{\partial(\Delta G_{el})}{\partial n_1} = \Delta\mu_{tot} = \Delta\mu_{mix} + \Delta\mu_{el} \quad (15)$$

In Eq. (15), $\Delta\mu_{mix}$ represents the chemical potential contribution of polymer-solvent mixing.

In addition to the updates to the elastic chemical potential described in section 2.3 (Eq. (10)), two advances have contributed to a more accurate understanding of swelling equilibrium in hydrogels. First, the polymer-solvent interaction parameter for polymer networks has been measured with increased accuracy, accounting for both the influence of polymer volume fraction and the differences between a polymer network and uncrosslinked polymer chains [39]. Second, additional chemical potential terms have been introduced for special cases. Among the additional chemical potential terms, the effect of an ionized solvent on a weak ionic polymer network has received the most theoretical and experimental development. The pH-dependent swelling behavior of weak ionic hydrogels has made them especially useful in controlled release applications [5,40,41].

3.2. Refining the polymer-solvent interaction parameter

The free energy of polymer-solvent mixing and the associated solvent chemical potential, first derived by Flory and Huggins [9], (Eqs. (16) and (17)) remain applicable in modern hydrogel characterization. However, since the polymer-solvent interaction parameter is a function of the polymer volume fraction [10,39], it cannot be represented as the same constant value when partially differentiated for the chemical potential equation. Therefore, $\tilde{\chi}$ is used in the free energy equation, and χ is used in the chemical potential equation. χ is then represented as a serial expansion with respect to polymer volume fraction (φ) (Eq. (18)). Typically, the first two coefficients (χ_0 and χ_1) are used since the polymer volume fraction-dependence is usually linear over the relevant range of polymer volume fractions [39]. Notably, the polymer-solvent interaction parameter is the average result of noncovalent and nonionic chemical interactions between the polymer and solvent, so it accounts for hydrogen bonding between the polymer network and

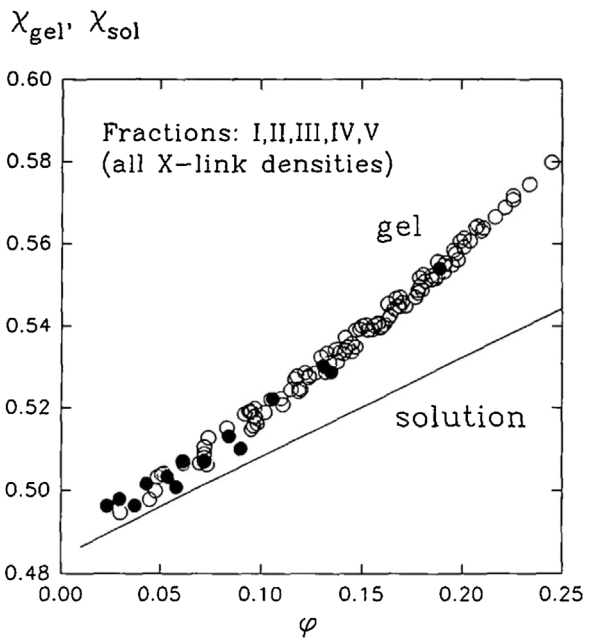

Fig. 4. Polymer-solvent interaction parameters χ_{gel} and χ_{sol} versus polymer volume fraction φ for PVA hydrogels (circles) and PVA/water solution (continuous line). The PVA gels were prepared from fractions I-V at different polymer concentrations: (●) fully swollen gels ($a_1 = 1$); (○) partially deswollen gels ($a_1 < 1$). [39], Copyright 1994. Reprinted with permission from Elsevier Science Ltd.

aqueous solution in hydrogels. It does not account for hydrogen bonding between two of the polymer network's repeating units, which would manifest as a higher-order mechanical contribution.

$$\Delta G_{mix} = k_b T[n_1 \ln(1-\varphi) + \bar{\chi} n_1 \varphi] \tag{16}$$

In Eq. (16), k_b is the Boltzmann thermodynamic constant.

$$\Delta \mu_{mix} = RT[\ln(1-\varphi) + \varphi + \chi\varphi^2] \tag{17}$$

$$\chi = \chi_0 + \chi_1\varphi + \chi_2\varphi^2 + \ldots \tag{18}$$

While the polymer-solvent interaction parameter was originally assumed to be identical for uncrosslinked polymers and polymer networks comprised of the same repeating units, the structural and chemical influences of crosslinking may reduce the effective affinity between polymer and solvent. McKenna and Horkay [39] used a combination of swelling and mechanical testing experiments to evaluate the polymer-solvent interaction parameter of PVA networks, finding that χ_0 and χ_1 differ for PVA networks and uncrosslinked PVA chains (Fig. 4). The mechanism driving these differences has not been determined and should be further validated on other hydrogel systems.

3.3. Ionic chemical potential contributions

Reversible pH-dependent swelling of weakly ionic hydrogels introduces a third chemical potential term for equilibrium swelling in hydrogels [42] (Eq. (19)). Like mixing and elastic contributions, the ionic term ($\Delta\mu_{ion}$) depends on the balance of solvent molecules inside and outside the polymer network system. The ionic chemical potential across the surface of the hydrogel scales with the concentration difference of positive and negative charges inside and outside the hydrogel (Eq. (20)).

$$\Delta\mu_{tot} = \Delta\mu_{mix} + \Delta\mu_{el} + \Delta\mu_{ion} \tag{19}$$

$$\frac{\Delta\mu_{ion}}{V_1 RT} = c^-_{gel} + c^+_{gel} - c^-_{sol} - c^+_{sol} \tag{20}$$

In Eq. (20), c^-_{gel} is the concentration of negative ions in the hydrogel, c^+_{gel} is the concentration of positive ions in the hydrogel, c^-_{sol} is the concentration of negative ions in the solution, and c^+_{sol} is the concentration of positive ions in the solution.

The dominant model for evaluating charge distributions between a hydrogel and its surroundings was adapted from Donnan theory for mobile ion distributions across semipermeable membranes (Fig. 5). Donnan equilibrium requires equivalent charge ratios for mobile ions (Eq. (21))

$$\frac{c^+_{m,sol}}{c^+_{m,gel}} = \frac{c^-_{m,gel}}{c^-_{m,sol}} \tag{21}$$

In Eq. (21), $c^+_{m,sol}$ is the concentration of mobile positive ions in the solution, $c^+_{m,gel}$ is the concentration of mobile positive ions in the hydrogel, $c^-_{m,gel}$ is the concentration of mobile negative ions in the hydrogel, and $c^-_{m,sol}$ is the concentration of mobile negative ions in the solution.

For the limited system of a simple anionic or cationic repeating unit in the polymer network and a 1:1 free electrolyte in solution, equation (20) can be solved analytically in terms of the solution's ionic strength (I) and the concentration of polymer-associated charges using Donnan equilibrium theory. First, for an excess of solution at ionic equilibrium outside the hydrogel, the concentration of ions in the solution is unaffected by the presence of the hydrogel, meaning that the mobile ion charge in the solvent and the total ion charge in the solvent are both equivalent to the ionic strength for a solution of 1:1 electrolytes (Eq. (22)).

$$c^+_{m,\,sol} = c^-_{m,\,sol} = c^-_{sol} = c^+_{sol} = I \tag{22}$$

Second, the ion concentration in a gel cannot be measured directly, but at equilibrium the total concentration of positive and negative charges within the hydrogel must be equal. For an anionic polymer network (signs would be inverted for a cationic polymer network), the total and mobile ion concentrations at equilibrium are related through Eq. (23).

$$c^+_{gel} = c^+_{m,\,gel} = c^-_{m,\,gel} + c^-_{polymer,\,gel} = c^-_{gel} \tag{23}$$

Third, the polymer-associated charge concentration, if there is one charged group per polymer repeating unit, can be calculated from the swollen polymer volume fraction (Eq. (24)).

$$c^-_{polymer,\,gel} = \frac{i\varphi_s\rho_d}{M_r} \tag{24}$$

In Eq. (24), i is the degree of ionization of the hydrogel and M_r is the molecular weight of the repeating unit.

Combining Eqs. (20)–(24) yields the ionic chemical potential term for swollen polymer networks that unites previous work by Flory [9], Brannon-Peppas and Peppas [42], and Horkay, Tasaki, and Basser [43,44] (Eq. (25)). A notable feature of the new ionic chemical potential term is stability at low ionic strength. The Brannon-Peppas ionic chemical potential term, by comparison, results in unrealistically high predictions of swelling ratio at low ionic strength (Fig. 6).

$$\frac{\Delta\mu_{ion}}{V_1 RT} = 2\left[I^2 + \left(\frac{i\varphi_s\rho_d}{2M_r}\right)^2\right]^{\frac{1}{2}} - 2I \tag{25}$$

For weakly ionic polymers such as poly(acrylic acid) (PAA) and poly(diethylaminoethyl methacrylate) (PDEAEMA), the degree of ionization (i) ranges from 0 to 1 based on the solution's pH. Weak anionic polymers become charged at high pH (Eq. (26)), and weak cationic polymers become charged at low pH (Eq. (27)). Notably,

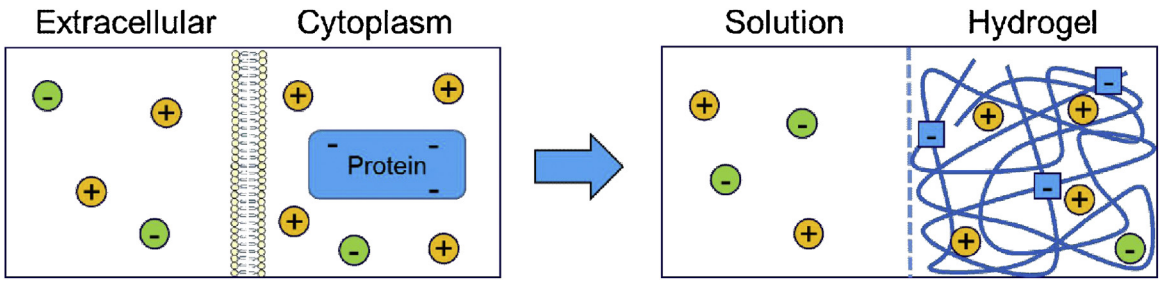

Fig. 5. Donnan equilibrium theory, originally developed for mobile ion distribution across cell membranes due to immobile protein-associated charges, applies in hydrogels with immobile network-associated charges.

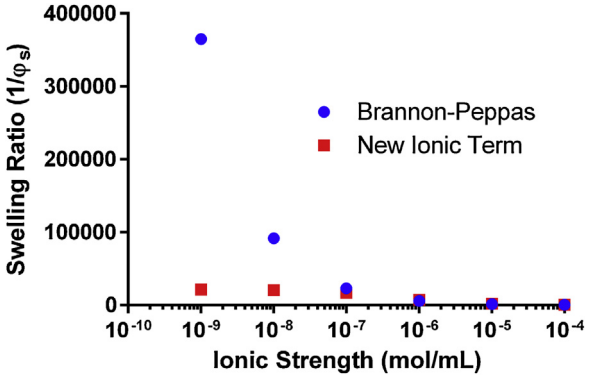

Fig. 6. The Brannon-Peppas ionic chemical potential term scales inversely with ionic strength and greatly overestimates the effect of low ionic strengths on hydrogel swelling. With the new ionic term, ionic strength has a logarithmic relationship, and low ionic strength has a limited effect on swelling. The new ionic term and the Brannon-Peppas term converge at high ionic strength. Data points are based on an idealized polymer network structure to demonstrate the isolated relationship between ionic strength and swelling ratio for each model.

neutral polymers always have a degree of ionization of zero, causing Eq. (25) to reduce to zero regardless of ionic strength.

$$i = \frac{K_a}{10^{-pH} + K_a} \tag{26}$$

In Eq. (26), K_a is the acid dissociation constant, and pH is the power of hydrogen or hydronium ion concentration ratio in aqueous solution.

$$i = \frac{K_b}{10^{-pOH} + K_b} \tag{27}$$

In Eq. (27), K_b is the base dissociation constant, and pOH is the power of hydroxide ion concentration ratio in aqueous solution.

Certainly, the requirements for 1:1 electrolyte solutions and simple ionic polymer repeating units limit application to polymer networks with complex charge distributions and to physiologically relevant buffered solutions. Notably, ionic hydrogel interactions with divalent ions such as calcium ions have the potential for transient ionic crosslinking or effectively permanent ionic crosslinking with trivalent ions [43,44]. Even within this simplified framework, there remains the confounding potential for counterion condensation at high electrolyte concentrations [43–46]. Furthermore, when considering this model in the full summation of chemical potentials at swelling equilibrium, the presence of electrolyte invalidates the assumption of a two-component system, creating an associated error in the mixing term. We anticipate that future research into the swelling of ionic polymer networks from the fundamental perspective of multiple chemical potentials will push past the limitations of the Donnan equilibrium theory approach and develop fundamental predictions for swelling behavior even in the context of buffered solutions and the presence of multivalent ions.

3.4. Other possible chemical potential terms

The current system of predicting swelling as the sum of chemical potential contributions does not exclude the possibility of other chemical potential terms beyond those described above. Horkay and colleagues proposed a term that accounts for the presence of densely crosslinked microclusters within an otherwise-homogeneous hydrogel [47]. Temperature-dependent solubility may warrant another term with similar behavior to the pH-associated ionic term. New hydrogel systems may produce new or significantly enhanced effects that could compete with the established chemical potential terms that guide the current understanding of hydrogel swelling. For incorporation into equilibrium swelling theory, these effects must be quantified and modeled as novel chemical potential terms or modifications to the existing chemical potential terms.

3.5. Prediction of molecular weight between crosslinks

From the summation of mixing chemical potential, elastic chemical potential, and ionic chemical potential at equilibrium, measurements of the polymer volume fraction in the relaxed state and the equilibrium swollen state enable prediction of the molecular weight between crosslinks ($\overline{M}_c$). (Eq. (28)).

$$\frac{1}{\overline{M}_c} = \frac{\ln(1-\varphi_s) + \varphi_s + \chi\varphi_s^2 - 2V_1\left[I^2 + \left(\frac{i\varphi_s\rho_d}{2M_r}\right)^2\right]^{\frac{1}{2}} + 2V_1 I}{-1^*\left(1-\frac{2}{f}\right)(1-\gamma)V_1\rho_d\varphi_r^{\frac{2}{3}}\varphi_s^{\frac{1}{3}}} \tag{28}$$

While equilibrium swelling theory provides a powerful tool for predicting the structure of a swollen polymer network, quantitative models of equilibrium swelling rely on many idealized and conditional assumptions, and by applying these equations to the analysis of real systems, a broad collection of theoretical and experimental errors may be incorporated in the results. However, equilibrium swelling theory corroborates many insightful studies about the mechanisms behind swollen polymer network behavior and contributed significantly to the design of advanced hydrogel systems. With ongoing improvements to address quickly expanding hydrogel synthesis capabilities, there is no doubt that equilibrium swelling theory will continue to guide precise design for a wide range of hydrogel systems.

4. Mesh size theory

4.1. Effective solute diffusivity in hydrogels

In addition to their mechanical and swelling properties, hydrogels are valued for their ability to modify the transport of solutes in aqueous solution [4,5,48]. In controlled release from a hydro-

gel reservoir, transport cannot be simplified to purely diffusive behavior since it is also affected by the chemical potential gradient, convective flow at the surface, and potential binding behavior between the polymer network and the solute. However, transport within the bulk of a homogeneous hydrogel can be assessed in terms of effective diffusivity since there is usually little to no convective flow, no chemical potential gradient at steady state, and binding behavior should be homogeneous within the system. In this regime, one may begin to assess what physical properties of the swollen polymer network and the solute affect the effective diffusivity of the solute within the hydrogel.

4.2. Experimental methods for studying mesh size theory

Two experimental techniques measure effective diffusivity of solutes in hydrogel without relying on release from the hydrogel to a sampling reservoir or creating an artificial chemical potential gradient. Fluorescence recovery after photobleach (FRAP) has become the most common technique for characterizing diffusivity of fluorescently labeled solutes within a hydrogel matrix [19,49–54]. In a typical FRAP experiment, a powerful laser photobleaches a region of the sample, and diffusivity is measured as an average result of the recovery of fluorescence within that region, primarily through Brownian motion of unbleached fluorescent molecules into the target area. FRAP is broadly applicable in that it can be performed on most confocal laser scanning microscopes and with any fluorescent probe capable of photobleaching. Similarly, the analysis has been optimized for a broad set of conditions, with the most powerful analysis technique for diffusion within hydrogels, developed by Jönsson et al. in 2008, readily available as a MATLAB program [49,55].

Fluorescence correlation spectroscopy (FCS) complements FRAP by correlating diffusivity coefficients from the residence times of fluorescent particles moving through a small, static illuminated volume [18,56–58]. As a result of the unchanging measurement position, this method is more sensitive to microscale heterogeneities in the hydrogel structure than FRAP. FCS does not need the high-powered laser used in FRAP, and data is collected at much lower fluorophore concentrations. However, FCS cannot resolve data from disperse solutes, rendering the dextran-conjugated fluorescein isothiocyanate (FITC-dextran) probe often used in FRAP and controlled release experiments unusable in FCS experiments. While FRAP is the more universal tool, FCS characterizes the diffusion of fluorescently labeled proteins through hydrogels with greater precision, which might make it more appropriate for studies that evaluate hydrogels as temporary replacements for damaged extracellular matrix. Increased use of both FRAP and FCS will improve the quality of data describing solute diffusion in hydrogels, leading to further refinement of mesh size theory and improved design of hydrogel-based extracellular matrix mimics and controlled release systems.

4.3. Evaluating mesh size from swelling data

The effects of a swollen polymer network on solute diffusivity are often discussed in terms of the mesh size (ξ), also known as the average correlation length of a chain in the swollen polymer network [19,28,33,59,60]. To date, no technique provides the resolution to directly measure mesh size without removing the solvent, so all analysis of mesh size has been performed by correlation. While the most powerful mesh size correlation technique may use small-angle neutron scattering [61], the most accessible technique is based upon interpretation of swelling data. This approach is popularly associated with Canal and Peppas [62], and the resulting equation has been called the Canal-Peppas equation (Eq. (29)).

$$\xi = \varphi_s^{-\frac{1}{3}} \left(l^2 C_n \frac{2\overline{M}_c}{M_r} \right)^{\frac{1}{2}} \tag{29}$$

In Eq. (29), l is the polymeric carbon-carbon bond length, and C_n is the polymer-specific characteristic ratio for a chain of n repeating units.

We propose several updates to improve the Canal-Peppas equation. As with the Peppas-Merrill equation, the Canal-Peppas assumes affine network behavior. Converting to a phantom network model introduces a functionality-dependent relaxation factor. For chains long enough to form Gaussian chain distributions, as previously assumed when deriving mechanical relationships, the characteristic ratio converges to C_∞, which is no longer dependent on the length of the chain. Additionally, the factor of two in the equation represents the two chain backbone bonds per repeating unit in a vinyl polymer. We generalize this value for non-vinyl polymers by replacing the two with a backbone bond factor (λ). As an example, PEG chains would have a backbone bond factor of 3. When the relevant bond length is no longer based only on carbon-carbon bonds, Flory recommended a weighted average of the bond lengths per repeating unit ($\bar{l}$) [9]. Including these changes produces a more accurate and universal version of the Canal-Peppas equation (Eq. (30)).

$$\xi = \varphi^{-\frac{1}{3}} \left(\left(1 - \frac{2}{f} \right) \bar{l}^2 C_\infty \frac{\lambda \bar{M}_c}{M_r} \right)^{\frac{1}{2}} \tag{30}$$

4.4. Hydrodynamic, free volume, and obstruction models

Any understanding of how solutes diffuse in a hydrogel must first address how solutes diffuse in water. The Stokes-Einstein equation [54] (Eq. (31)) describes solute diffusion in a solvent without net fluid flow based on the solute's effective radius (r_s) and the solvent's viscosity (η). In mesh size theory, Eq. (31) is used to calculate D_0, the diffusivity coefficient of the solute in water. Basic hydrodynamic models such as the Cukier model describe scaling corrections to the diffusivity coefficient of solutes in a mixture of polymer and solvent [63].

$$D_0 = \frac{k_b T}{6\pi\eta r_s} \tag{31}$$

By expanding upon hydrodynamic models with additional considerations for the physical effects of swollen polymer networks, two competing models have dominated discussion of mesh size theory, each with significant experimental and theoretical support acquired over decades of study. The free volume model, introduced by Peppas and colleagues [14,64], presents the swollen polymer network as a dynamic lattice structure that yields transient free volumes that solutes can diffuse through if their trajectory aligns with the available free volume. In the scaling free volume model of Lustig and Peppas [65] (Eq. (32)), mesh size acts as a limiting factor to the size of the solute that can pass through the network, and polymer volume fraction correlates to the probability of a solute interacting with the polymer network as it moves within the hydrogel. The scale factor Y results from the free volume-normalized volume displacement for each diffusional jump and therefore may be approximated as unity [65]. Notably, this free volume model predicts nonphysical negative diffusivities for solutes whose radii exceed the mesh size, clearly indicating that broad practical application of the free volume model would require further development and system-specific analysis to ground the scaling relationship.

$$\frac{D}{D_0} \cong \left[1 - \frac{r_s}{\xi} \right] \exp\left[-Y^* \frac{\varphi}{1-\varphi} \right] \tag{32}$$

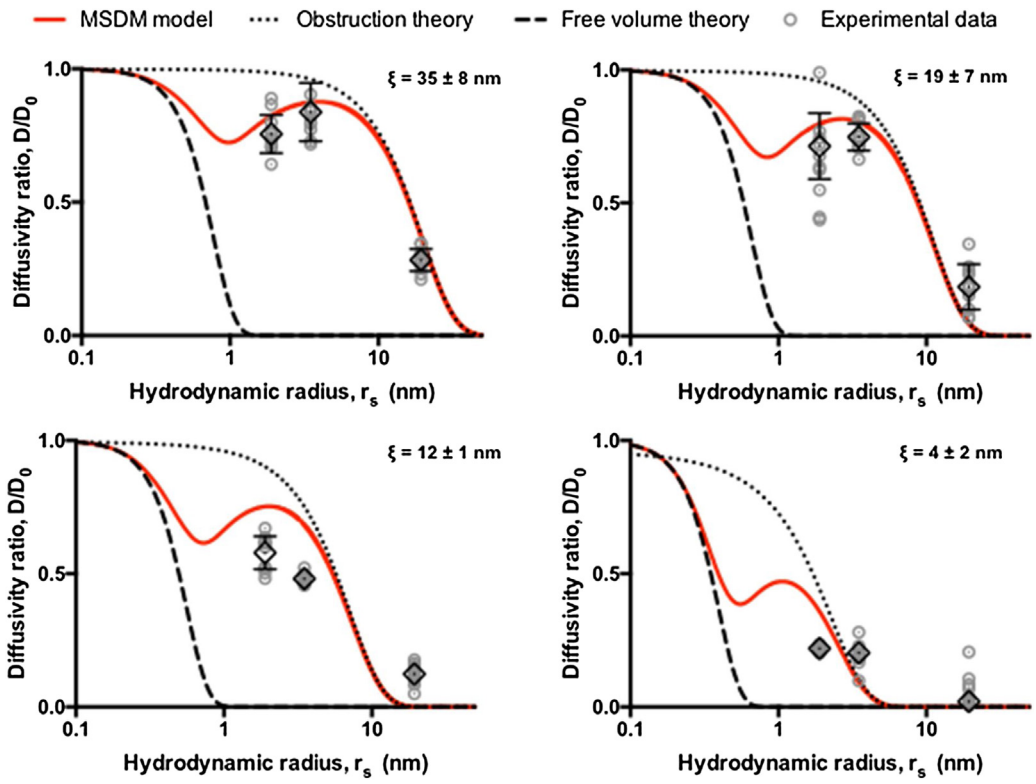

Fig. 7. Normalized diffusivities predicted by the multiscale diffusion model (MSDM) compared against experimentally obtained values. Experimental data (gray circles; error bars denote mean ± s.d.; $n = 10$) and theoretical predictions (lines) for the normalized diffusivity, D/D_0, versus solute hydrodynamic radius (r_s) for poly(ethylene glycol) (PEG) hydrogels with different mesh sizes (ξ; mean ± s.d.; $n = 4$). The MSDM model (red solid line) predicts the existence and location of a local minimum and maximum in D/D_0, whereas free volume theory (black dashed line) and obstruction theory (black dotted line) do not. These local minima/maxima in D/D_0 are reflected in the experimental data. [15], Copyright 2019. Reprinted with permission.

In Eq. (32), D represents the diffusivity of the solute within the swollen polymer network.

The competing obstruction scaling model, initially developed by Ogston et al., [66] evaluates the polymer chains in the network as relatively large fibers that obstruct solute motion. As such, the mesh size is assumed to be too large to have an effect, and solute diffusivity scales with the fiber radius (r_f) and the polymer volume fraction (Eq. (33)).

$$\frac{D}{D_0} = \exp\left[\frac{-(r_s + r_f)}{r_f}\varphi^{\frac{1}{2}}\right] \tag{33}$$

Perhaps because solute transport in hydrogels is such a critical issue in several biomedical applications, many groups have independently attempted to improve the quantitative models following Ogston and Peppas. Amsden provided an extensive review of quantitative models developed before 1998 [16], broadly classifying the models for application to homogeneous or heterogeneous hydrogels based on the polymer network's rigidity. A following review by Masaro and Zhu [67] discusses the existing models within the theoretical categories of obstruction models, hydrodynamic models, and free volume models.

Following these comprehensive reviews, Amsden developed an obstruction model that incorporated mesh size [68]. Recently, Axpe et al. coordinated the Amsden model and the free volume model to form the multiscale diffusion model in an attempt to continuously estimate solute diffusivity in hydrogels as solute sizes scale from near the size of the polymer fiber radius to near and above the mesh size [15] (Eq. (34)). Notably, the multiscale diffusion model captures a local spike in normalized diffusivity that occurs at the transition between the dominant length scales (Fig. 7), though this result should be further tested with FRAP and FCS on a broad range of hydrogel systems and solutes to validate its universality. The key experimental technique supporting the multiscale diffusion model is the characterization of free volume spaces using positron annihilation lifetime spectroscopy (PALS). According to Axpe et al., the radius of free volume spaces in a swollen polymer network (r_{FV}) determines the extent to which solutes diffuse through a free volume mechanism or an obstruction-limited mechanism. Like the simplifying assumption that $Y = 1$ in the free volume model, Axpe et al., suggest that the free volume radius in hydrogels may be approximated as the free volume radius in water ($r_{FVW} = 0.269$ nm) in the absence of PALS data.

$$\frac{D}{D_0} = erf\left(\frac{r_{FV}}{r_s}\right)\exp\left[-1^*\left(\frac{r_s}{r_{FVW}}\right)^3\left(\frac{\varphi}{1-\varphi}\right)\right] + erfc\left(\frac{r_{FV}}{r_s}\right)\exp\left[-\pi^*\left(\frac{r_s + r_f}{\xi + 2r_f}\right)^2\right] \tag{34}$$

As noted by the authors, this multiscale diffusion model still fails to address the influences of shape in the solute, the free volume void spaces, and the mesh openings presented by the polymer network. However, this was the first study to theoretically and experimentally resolve long-standing inconsistencies between free volume models and obstruction models, marking a milestone in the development of mesh size theory.

4.5. Further questions in mesh size theory

Despite the convergence of models described above, several factors affecting solute diffusion in hydrogels remain 'open questions' in mesh size theory. While the various models thoroughly address the effects of size and scale, solute shape and network topology

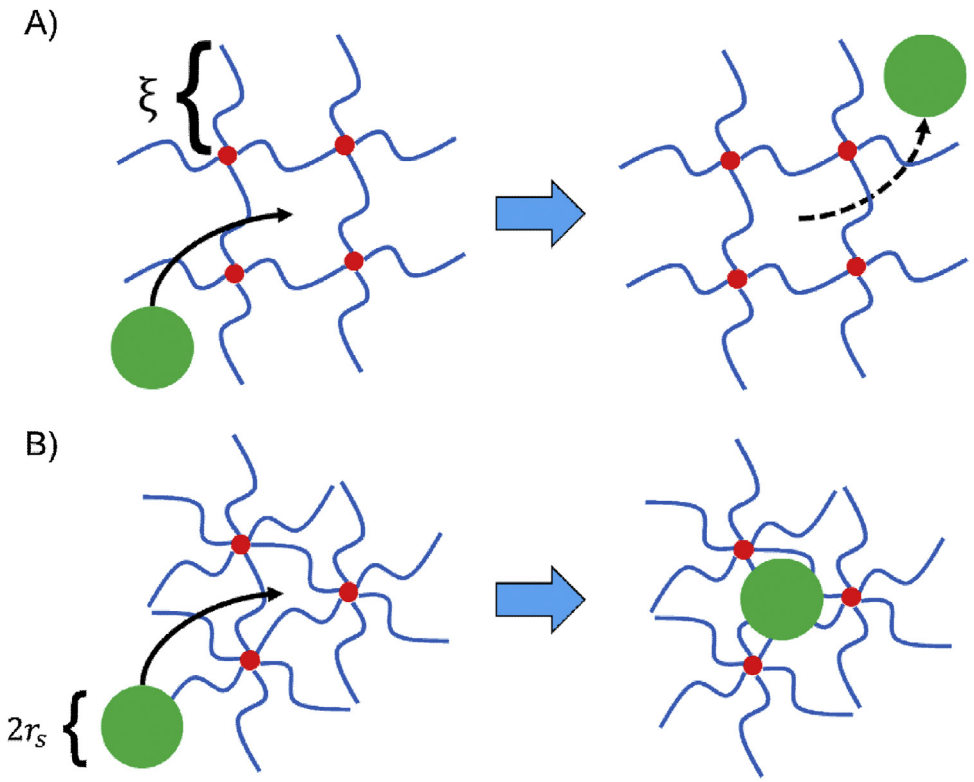

Fig. 8. Even with equivalent mesh sizes, junction functionality affects whether a solute can diffuse through a swollen polymer network. A) The first hydrogel system has tetrafunctional junctions and enables the solute to pass through its void space. B) The second hydrogel system has hexafunctional junctions, and the resulting network structure blocks the solute's motion.

should cause significant effects, especially when the size of the solute is similar to the mesh size. The Stokes-Einstein equation sets the precedent for ignoring solute shape by approximating all solutes as hard spheres, but the flexible polymer-based reptation model of diffusion discussed by de Gennes [69] suggests that mesh size theory could be updated for a variety of solute shapes.

Network topology can be initially addressed by updating the model with junction functionality-associated scaling parameters. To understand the effect network topology might have on solute diffusivity, consider two swollen polymer networks. They have equivalent mesh sizes, but one has a junction functionality of four and the other has a junction functionality of six. The network structure that the solutes diffuse through will have more angular openings in the higher functionality network, leading to a greater probability of immobilizing the solute (Fig. 8). How significantly solute diffusivity would change in response to junction functionality is unclear and may require further insightful experimental studies to establish trends fit for modeling.

As the mesh size theory models become more precise and comprehensive, lesser contributions of statistical mechanics or additional system-specific properties will become relevant, especially if mesh size theory follows the developmental trends of rubberlike elasticity theory and equilibrium swelling theory. The effects of bulky side groups and complex chain structures (Fig. 3) must also be modeled in mesh size theory, possibly with the same methods that may eventually arise for rubberlike elasticity theory and equilibrium swelling theory. Obstruction models partially incorporate the bulkiness of side groups in the fiber radius term, but even this approach may be missing some of the nuance associated with side-group structure, such as in cases of copolymers with a bulky repeating unit and a narrow repeating unit.

Discussion toward a universal model for solute diffusion within hydrogels would not be comprehensive without addressing the complex chemical interactions of a three-part solute-solvent-network system. These interactions are far less universally tractable than the questions of size and shape, which has led many researchers in the field to use polymers and solutes that minimize chemical interactions, such as PEG and FITC-dextran [21,50,52,54,70]. However, many of the most interesting properties of biotransport rely on reversible binding between the polymer and solute, such as cytokine sequestration by extracellular matrix components. Though equations have been developed for these conditions, they rapidly increase in complexity and therefore have not seen widespread adoption [71]. For example, Sakiyama-Elbert and Hubbell developed a model of heparin-bound growth factor release that requires simultaneous solution of six differential equations with three separate diffusivity coefficients [72]. Rossi et al., describe a combined diffusion and adsorption model, but the influence of the gel structure is modeled as a general porosity term [73]. Additionally, ionized hydrogels may provide an alternative transport mechanism for ionic solutes, wherein solutes travel faster or slower than free diffusion when carried along charged polymer chains [45,46,74]. Current fundamental models either ignore these effects, creating systematic errors, or average them into the overall effective diffusivity, making the model more empirical. Future models of mesh size theory will need to efficiently characterize chemical factors and mechanisms of solute transport in hydrogels.

5. Conclusions

Here we present updates to three fundamental theories relating structure and function in hydrogels through the uniting perspective of the swollen polymer network hypothesis.

While the equations described in this review include extensive assumptions and unrealistic generalizations about swollen polymer networks, they also formalize a deep body of accumulated theoretical and experimental knowledge on polymer network properties. Unlike simulated and machine learning approaches, the

formal modeling approach provides clear and specific opportunities for improvement and a logical, fundamental basis for each component. In reviewing the current state of the polymer network hypothesis, we record a benchmark in the ongoing process and anticipate further refinement in both accuracy and breadth of application.

Eqs. (14), (28), (31), and (34) reveal the extensive parallelism between swelling, mechanical, and diffusive properties in hydrogels. Taken together, these equations indicate that a hydrogel's swelling data could be used to predict the hydrogel's stiffness and the diffusivity of solutes within the hydrogel.

In hydrogel quantitative modeling, issues of size and scale have made considerable progress. Hydrogel stiffness scales with the number of chains as originally suggested by rubberlike elasticity theory, but with additional considerations of the phantom-like network model, chain-end defects, and the effects of solvent dilution during synthesis. Equilibrium swelling, when modeled as the result of additive chemical potential terms, interprets the influences of polymer and solvent mixing, chain elasticity, and ionic charges from fundamental thermodynamic relationships. The multiscale diffusivity model predicts solute transport in hydrogels based on the relative sizes of the solutes, free volume voids, and the hydrogel's mesh.

Looking forward, the greatest questions remain in shape and higher-order interactions. How do bulky and complex polymer repeating units affect swollen polymer networks? What can be learned about swollen polymer network behavior by isolating the effects of junction functionality? To what extent does the swollen polymer network hypothesis apply to natural biopolymer systems such as gelatin or alginate hydrogels? The answers to these questions will be critical in developing fundamental models for the physical properties of the next generation of precision hydrogel biomaterials.

CRediT authorship contribution statement

Nathan R. Richbourg: Conceptualization, Methodology, Formal analysis, Writing - original draft, Writing - review & editing, Visualization. **Nicholas A. Peppas:** Conceptualization, Writing - review & editing, Supervision.

Declaration of Competing Interest

The authors declare that they have no known competing financial interests or personal relationships that could have appeared to influence the work reported in this paper.

Acknowledgements

While preparing this publication, NRR was supported by the National Science Foundation Graduate Research Fellowship Program, Grant No. DGE–161040.

References

[1] Peppas NA, Slaughter BV, Kanzelberger MA. Hydrogels. In: Matyjaszewski K, Möller M, editors. Polymer science: a comprehensive reference. Amsterdam: Elsevier; 2012. p. 385–95.
[2] Culver HR, Sharma I, Wechsler ME, Anslyn EV, Peppas NA. Charged poly(N-isopropylacrylamide) nanogels for use as differential protein receptors in a turbidimetric sensor array. Analyst 2017;142:3183–93.
[3] Culver HR, Clegg JR, Peppas NA. Analyte-responsive hydrogels: intelligent materials for biosensing and drug delivery. Acc Chem Res 2017;50:170–8. Erratum op. cit. 2018;51:2600-0.
[4] Li J, Mooney DJ. Designing hydrogels for controlled drug delivery. Nat Rev Mater 2016;1, 16071/1-17.
[5] Sharpe LA, Daily AM, Horava SD, Peppas NA. Therapeutic applications of hydrogels in oral drug delivery. Expert Opin Drug Deliv 2014;11:901–15.
[6] Brown TE, Anseth KS. Spatiotemporal hydrogel biomaterials for regenerative medicine. Chem Soc Rev 2017;46:6532–52.
[7] Slaughter BV, Khurshid SS, Fisher OZ, Khademhosseini A, Peppas NA. Hydrogels in regenerative medicine. Adv Mater 2009;21:3307–29.
[8] Gu Y, Zhao J, Johnson JA. Polymer networks: from plastics and gels to porous frameworks. Angew Chem Int Ed 2020;59:5022–49.
[9] Flory PJ. Principles of polymer chemistry. In: Rubberlike elasticity. Ithaca: Cornell University Press; 1953, 688 pp.
[10] Erman B, Mark JE. Structures and properties of rubberlike networks. Oxford: Oxford University Press; 1997, 369 pp.
[11] Treloar LRG. The physics of rubber elasticity. Oxford: Oxford University Press; 1975, 324 pp.
[12] Flory PJ, Rehner J. Statistical mechanics of cross-linked polymer networks II. Swelling. J Chem Phys 1943;11:521–6.
[13] Flory PJ, Rehner J. Statistical mechanics of cross-linked polymer networks I. J Chem Phys 1943;11:512–20.
[14] Peppas NA, Reinhart CT. Solute diffusion in swollen membranes. Part I. A new theory. J Membr Sci 1983;15:275–87.
[15] Axpe E, Chan D, Offeddu GS, Chang Y, Merida D, Hernandez HL, et al. A multiscale model for solute diffusion in hydrogels. Macromolecules 2019;52:6889–97.
[16] Amsden B. Solute Diffusion within Hydrogels. Mechanisms and Models. Macromolecules 1998;31:8382–95.
[17] Offeddu GS, Axpe E, Harley BAC, Oyen ML. Relationship between permeability and diffusivity in polyethylene glycol hydrogels. AIP Adv 2018;8, 105006/1-7.
[18] Zustiak SP, Boukari H, Leach JB. Solute diffusion and interactions in cross-linked poly(ethylene glycol) hydrogels studied by Fluorescence Correlation Spectroscopy. Soft Matter 2010;6:3609–18.
[19] Hagel V, Haraszti T, Boehm H. Diffusion and interaction in PEG-DA hydrogels. Biointerphases 2013;8, 36/1-10.
[20] Peppas NA, Merrill EW. Crosslinked poly(vinyl alcohol) hydrogels as swollen elastic networks. J Appl Polym Sci 1977;21:1763–70.
[21] Browning MB, Wilems T, Hahn M, Cosgriff-Hernandez E. Compositional control of poly(ethylene glycol) hydrogel modulus independent of mesh size. J Med Polym Sci Part A 2011;(98A):268–73.
[22] Flory PJ. Theory of elasticity of polymer networks. The effect of local constraints on junctions. J Chem Phys 1977;66:5720–9.
[23] James HM. Statistical properties of networks of flexible chains. J Chem Phys 1947;15:651–68.
[24] James HM, Guth E. Statistical thermodynamics of rubber elasticity. J Chem Phys 1953;21:1039–49.
[25] Deam RT, Edwards SF. The theory of rubber elasticity. Philos Trans A Math Phys Sci 1976;280:317–53.
[26] Barr-Howell BD, Peppas NA. Importance of junction functionality in highly crosslinked polymers. Polym Bull (Berl) 1985;13:91–6.
[27] Kim J, Kong YP, Niedzielski SM, Singh RK, Putnam AJ, Shikanov A. Characterization of the crosslinking kinetics of multi-arm poly(ethylene glycol) hydrogels formed via Michael-type addition. Soft Matter 2016;12:2076–85.
[28] Jimenez-Vergara AC, Lewis J, Hahn MS, Munoz-Pinto DJ. An improved correlation to predict molecular weight between crosslinks based on equilibrium degree of swelling of hydrogel networks. J Med Polym Sci Part B 2017;106:1339–48.
[29] Kaga S, Arslan M, Sanyal R, Sanyal A. Dendrimers and Dendrons as versatile building blocks for the fabrication of functional hydrogels. Molecules 2016;21, 497/1-25.
[30] Zhou H, Woo J, Cok AM, Wang M, Olsen BD, Johnson JA. Counting primary loops in polymer gels. Proc Natl Acad Sci U S A 2012;109:19119–24.
[31] Lin T-S-S, Wang R, Johnson JA, Olsen BD. Revisiting the elasticity theory for real gaussian phantom networks. Macromolecules 2019;52:1685–94.
[32] Flory PJ. Statistical mechanics of swelling of network structures. J Chem Phys 1950;18:108–11.
[33] Rehmann MS, Skeens KM, Kharkar PM, Ford EM, Maverakis E, Lee KH, et al. Tuning and predicting mesh size and protein release from step growth hydrogels. Biomacromolecules 2017;18:3131–42.
[34] Bray JC, Merrill EW. Poly(vinyl alcohol) hydrogels. Formation by electron beam irradiation of aqueous solutions and subsequent crystallization. J Appl Polym Sci 1973;17:3779–94.
[35] Anseth KS, Bowman CN, Brannon-Peppas L. Mechanical properties of hydrogels and their experimental determination. Biomaterials 1996;17:1647–57.
[36] Mark JE, Erman B. Rubberlike elasticity: a molecular primer. Cambridge: Cambridge University Press; 2007, 213 pp.
[37] Flory PJ. Statistical mechanics of chain molecules. New York: Interscience; 1980, 432 pp.
[38] Peppas NA, Moynihan HJ, Lucht LM. The structure of highly crosslinked poly(2-hydroxyethyl methacrylate) hydrogels. J Med Polym Sci 1985;19:397–411.
[39] McKenna GB, Horkay F. Effect of crosslinks on the thermodynamics of poly(vinyl alcohol) hydrogels. Polymer 1994;35:5737–42.
[40] Culver H, Daily A, Khademhosseini A, Peppas N. Intelligent recognitive systems in nanomedicine. Curr Opin Chem Eng 2014;4:105–13.
[41] Gao X, He C, Xiao C, Zhuang X, Chen X. Biodegradable pH-responsive polyacrylic acid derivative hydrogels with tunable swelling behavior for oral delivery of insulin. Polymer 2013;54:1786–93.

[42] Brannon-Peppas L, Peppas NA. Equilibrium swelling behavior of pH-sensitive hydrogels. Chem Eng Sci 1991;46:715–22.
[43] Horkay F, Tasaki I, Basser PJ. Effect of monovalent–divalent cation exchange on the swelling of polyacrylate hydrogels in physiological salt solutions. Biomacromolecules 2001;2:195–9.
[44] Horkay F, Tasaki I, Basser PJ. Osmotic swelling of polyacrylate hydrogels in physiological salt solutions. Biomacromolecules 2000;1:84–90.
[45] Kamcev J, Paul DR, Manning GS, Freeman BD. Ion diffusion coefficients in ion exchange membranes: significance of counterion condensation. Macromolecules 2018;51:5519–29.
[46] Kamcev J, Paul DR, Freeman BD. Ion activity coefficients in ion exchange polymers: applicability of Manning's counterion condensation theory. Macromolecules 2015;48:8011–24.
[47] Horkay F, Han MH, Han IS, Bang IS, Magda JJ. Separation of the effects of pH and polymer concentration on the swelling pressure and elastic modulus of a pH-responsive hydrogel. Polymer 2006;47:7335–8.
[48] Annabi N, Tamayol A, Uquillas JA, Akbari M, Bertassoni LE, Cha C, et al. 25th anniversary article: rational design and applications of hydrogels in regenerative medicine. Adv Mater 2013;26:85–124.
[49] Lorén N, Hagman J, Jonasson JK, Deschout H, Bernin D, Cella-Zanacchi F, et al. Fluorescence recovery after photobleaching in material and life sciences: putting theory into practice. Q Rev Biophys 2015;48:323–87.
[50] Hadjiev NA, Amsden BG. An assessment of the ability of the obstruction-scaling model to estimate solute diffusion coefficients in hydrogels. J Control Release 2015;199:10–6.
[51] Deschout H, Raemdonck K, Demeester J, De Smedt SC, Braeckmans K. FRAP in pharmaceutical research: practical guidelines and applications in drug delivery. Pharm Res 2014;31:255–70.
[52] Brandl F, Kastner F, Gschwind RM, Blunk T, Teßmar J, Göpferich A. Hydrogel-based drug delivery systems: comparison of drug diffusivity and release kinetics. J Control Release 2010;142:221–8.
[53] Branco MC, Pochan DJ, Wagner NJ, Schneider JP. Macromolecular diffusion and release from self-assembled β-hairpin peptide hydrogels. Biomaterials 2009;30:1339–47.
[54] Kosto KB, Deen WM. Diffusivities of macromolecules in composite hydrogels. AIChE J 2004;50:2648–58.
[55] Jönsson P, Jonsson MP, Tegenfeldt JO, Höök F. A method improving the accuracy of fluorescence recovery after photobleaching analysis. Biophysical J 2008;95:5334–48.
[56] Hess ST, Huang S, Heikal AA, Webb WW. Biological and chemical applications of fluorescence correlation spectroscopy: a review. Biochemistry 2002;41:697–705.
[57] Fatin-Rouge N, Starchev K, Buffle J. Size effects on diffusion processes within agarose gels. Biophysical J 2004;86:2710–9.
[58] Vagias A, Košovan P, Koynov K, Holm C, Butt HJ, Fytas G. Dynamics in Stimuli-Responsive Poly(N-isopropylacrylamide) hydrogel layers As revealed by fluorescence correlation spectroscopy. Macromolecules 2014;47:5303–12.
[59] Tsuji Y, Li X, Shibayama M. Evaluation of mesh size in model polymer networks consisting of tetra-arm and linear poly(ethylene glycol)s. Gels 2018;4, 50/1-12.
[60] Wisniewska MA, Seland JG, Wang W. Determining the scaling of gel mesh size with changing crosslinker concentration using dynamic swelling, rheometry, and PGSE NMR spectroscopy. J Appl Polym Sci 2018;135, 46695/1-10.
[61] Horkay F, Hecht A-M-M, Geissler E. Small angle neutron scattering in poly(vinyl alcohol) hydrogels. Macromolecules 1994;27:1795–8.
[62] Canal T, Peppas NA. Correlation between mesh size and equilibrium degree of swelling of polymeric networks. J Med Polym Sci 1989;23:1183–93.
[63] Cukier RI. Diffusion of Brownian spheres in semidilute polymer solutions. Macromolecules 1984;17:252–5.
[64] Reinhart CT, Peppas NA. Solute diffusion in swollen membranes. Part II. Influence of crosslinking on diffusive properties. J Membr Sci 1984;18:227–39.
[65] Lustig SR, Peppas NA. Solute diffusion in swollen membranes. IX. Scaling laws for solute diffusion in gels. J Appl Polym Sci 1988;36:735–47.
[66] Ogston AG, Preston BN, Wells JD, Snowden JM. On the transport of compact particles through solutions of chain-polymers. Proc R Soc Lond A Math Phys Sci 1973;333:297–316.
[67] Masaro L, Zhu XX. Physical models of diffusion for polymer solutions, gels and solids. Prog Polym Sci 1999;24:731–75.
[68] Amsden B. An obstruction-scaling model for diffusion in homogeneous hydrogels. Macromolecules 1999;32:874–9.
[69] De Gennes PG. Scaling concepts in polymer physics Ithaca. Cornell University Press; 1979, 323 pp.
[70] Sakai T, Matsunaga T, Yamamoto Y, Ito C, Yoshida R, Suzuki S, et al. Design and fabrication of a high-strength hydrogel with ideally homogeneous network structure from tetrahedron-like macromonomers. Macromolecules 2008;41:5379–84.
[71] Lin CC, Metters AT. Hydrogels in controlled release formulations: network design and mathematical modeling. Adv Drug Deliv Rev 2006;58:1379–408.
[72] Sakiyama-Elbert SE, Hubbell JA. Development of fibrin derivatives for controlled release of heparin-binding growth factors. J Control Release 2000;65:389–402.
[73] Rossi F, Castiglione F, Ferro M, Marchini P, Mauri E, Moioli M, et al. Drug–polymer interactions in hydrogel-based drug-delivery systems: an experimental and theoretical study. ChemPhysChem 2015;16:2818–25.
[74] Kamcev J, Paul DR, Manning GS, Freeman BD. Accounting for frame of reference and thermodynamic non-idealities when calculating salt diffusion coefficients in ion exchange membranes. J Membr Sci 2017;537:396–406.